J Mater Sci (2012) 47:308–314
DOI 10.1007/s10853-011-5799-7

Thermodynamic interaction and mechanical characteristics of Nylon 6 and polyhedral oligomeric silsesquioxane nanohybrids

Sang-Kyun Lim · Eun-Pyo Hong · Yu-Hyun Song · Hyoung Jin Choi · In-Joo Chin

Received: 11 May 2011 / Accepted: 15 July 2011 / Published online: 26 July 2011

Abstract Polyhedral oligomeric silsesquioxane (POSS) reagents have unique hybrid chemical compositions containing nano-sized cage structures with dimensions comparable to those of most polymer segments and coils. This article reports a generalized functionalization scheme of POSS that is suitable as a nanohybrid with Nylon 6. The thermodynamic interaction energy density, thermodynamic solubility parameter, and activation energy of the specific interaction between Nylon 6 and POSS were examined. The mechanical, thermal, and morphological properties of the Nylon 6 nanohybrids were also analyzed and compared with the theoretical estimation.

Introduction

A polymeric nanohybrid can be defined as a polymer filled with nanofillers, at least one of whose dimensions are in the nanometer range from 1 to 100 nm. These nanohybrids have attracted considerable interest in recent years. Nanofillers improve the mechanical, barrier, electrical, and thermal properties of base polymers significantly at a very low filler concentration compared to conventional macrocomposites. This has opened up possibilities for producing high-performance lightweight hybrids without compromising the other properties, such as optical behavior or weight. Carbon nanotubes/fibers, nanosilica, graphene, and nanoclays are currently the preferred fillers [1–7].

However, a new class of nanofiller, polyhedral oligomeric silsesquioxane (POSS), has emerged for use in nanostructured materials recently. Silsesquioxane is the term for all structures with the formula $(RSiO_{1.5})_n$, where R is hydrogen or any alkyl, alkylene, aryl, arylene, or organofunctional derivative of alkyl, alkylene, aryl, or arylene group [8–10]. Silsesquioxanes can form ladder [11], cage [12, 13], partial cage [14], and polymer structures [15]. Among the various types of silsesquioxanes, POSS, which is essentially an organic–inorganic hybrid material, contains a basic polyhedral silicon–oxygen nanostructured skeleton or cage, with a precisely defined Si–Si diameter of 0.53 nm. The cage may contain 8 (a cube-like cage) or 12 Si atoms located at the corner of the cage, surrounded by 8 or 12 organic groups, respectively [8]. The POSS chemistry is quite versatile, and it is possible to attach different functional or nonfunctional organic groups (R) to the corner Si molecules for further reactions. These organic groups can make these POSS molecules compatible with polymers or monomers. Such covalent POSS incorporation can lead to substantial improvements in polymer properties, including increases in the operation temperature, oxidation resistance, surface hardening, and mechanical properties, as well as decreases in flammability, heat evolution, and viscosity during processing [16–23]. POSS nanostructured chemicals can be incorporated into common polymers via coordination polymerization [24], ring-opening metathesis polymerization [25], conventional free radical polymerization [26], living/controlled free radical polymerization [27], condensation polymerization [28],

---

S.-K. Lim · E.-P. Hong · Y.-H. Song · H. J. Choi (✉) ·
I.-J. Chin (✉)
Department of Polymer Science and Engineering,
Inha University, Incheon 402-751, Korea
e-mail: hjchoi@inha.ac.kr

I.-J. Chin
e-mail: ichin@inha.ac.kr

S.-K. Lim
IBM Almaden Research Center, 650 Harry Road, San Jose,
CA 95120, USA

melt mixing [29–31], and hybrid systems along with other fillers [32], etc.

While considerable effort has been focused on the development of new POSS-containing nanohybrids as high-performance materials, reports on the specific interaction between the polymer matrix and POSS are seldom found. This study examined the thermodynamic interaction of binary components in nanohybrids containing a few percent of POSS nanoparticles, which were functionalized with aminopropylisobutyl-, aminopropylisooctyl-, or aminopropylphenyl groups, in a Nylon 6 matrix. The thermodynamic interaction was described by the thermodynamic interaction energy density based on the classical Flory–Huggins theory using the melting point depression method [33, 34]. The thermodynamic solubility parameters of Nylon 6 and the functionalized-POSS were evaluated to determine the Flory–Huggins interaction parameter based on the method reported by Hoftyzer and Van Krevelen, and Hoy. The interaction between Nylon 6 and POSS was also characterized by measuring the activation energy using the Kissinger method.

Experimental

Materials and preparation method

Nylon 6 was purchased from the Aldrich Chemical Co. The POSS nanoparticles, aminopropylisobutyl-POSS ($C_{31}H_{71}NO_{12}Si_8$, $F_W = 874.58$, denoted as AB), aminopropylisooctyl-POSS ($C_{59}H_{127}NO_{12}Si_8$, $F_W = 1267.32$, denoted as AO), and aminopropylphenyl-POSS ($C_{45}H_{43}NO_{12}Si_8$, $F_W = 1014.52$, denoted as AP), were purchased from Hybrid Plastics Inc., and were used as received. Figure 1 shows the chemical structures of the POSS-derivatives. Nylon 6 nanohybrids with POSS were prepared using the melt mixing method. After melting Nylon 6 at 230 °C using a torque rheometer (Plastograph EC, Brabender, Germany), the POSS was added at concentrations of 0.5, 1, and 2 wt% and mixed for 10 min.

FE-SEM and FT-TEM observations and mechanical analysis

The microstructure and elemental compositions of the dispersive POSS nanoparticles in the Nylon 6 matrix were examined by field-emission scanning electron microscopy (FE-SEM, S-4300, Hitachi, Japan) with an attached X-ray energy dispersive spectrometer (EDX) (E-1030, Horiba, UK). The samples for FE-SEM were coated with gold before the FE-SEM measurements. The electron beam spot size used in the EDX was approximately 5 nm in diameter. Field-emission transmission electron microscopy (FE-TEM, JEM 2100F, JEOL, Japan) was performed at an accelerated voltage of 100 kV. All ultrathin sections (less than 3 μm) were microtomed using an ultramicrotome (RMC-MTX, USA) with a diamond knife and observed by FE-TEM without staining. The mechanical properties of the Nylon 6/POSS nanohybrid films were examined using the uniaxial elongation method on a universal test machine (UTM, Hounsfield Test Equipment, UK) at room temperature. The sample size had typical dimensions of 10 mm (wide) × 50 mm (length) × 0.1 mm (thickness).

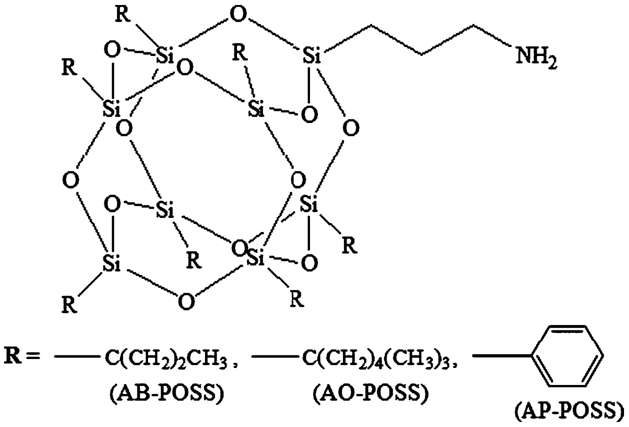

Fig. 1 The chemical structures of the POSS-derivatives

Thermodynamic interaction energy density and activation energy

Differential scanning calorimetry (DSC) (Pyris Diamond DSC, Perkin-Elmer, USA) was used to determine the interaction energy density of the Nylon 6/POSS nanohybrids by monitoring the change in the melting point. To measure the equilibrium temperature (T_m^0), the sample was heated to 240 °C, maintained at that temperature for 5 min to insure complete melting of the Nylon 6 crystals, quenched to the crystallization temperature at a cooling rate of 150 °C min^{-1}, T_c ($T_{c,1} = 185$ °C, $T_{c,2} = 190$ °C, $T_{c,3} = 195$ °C, and $T_{c,4} = 200$ °C), kept at T_c for at least 30 min, and then heated at a heating rate of 20 °C min^{-1}. The thermal stability of the nanohybrid was examined by thermogravimetric analysis (TGA, Q50, TA Instruments, USA). The samples were also heated to 750 °C at heating rates of 10, 20, and 40 °C min^{-1} with air purging to estimate the activation energy.

Results and discussion

Characterization of the POSS dispersion in the nanohybrids

The nanostructure formation of Nylon 6/POSS nanohybrids was examined by X-ray EDX mapping analysis using

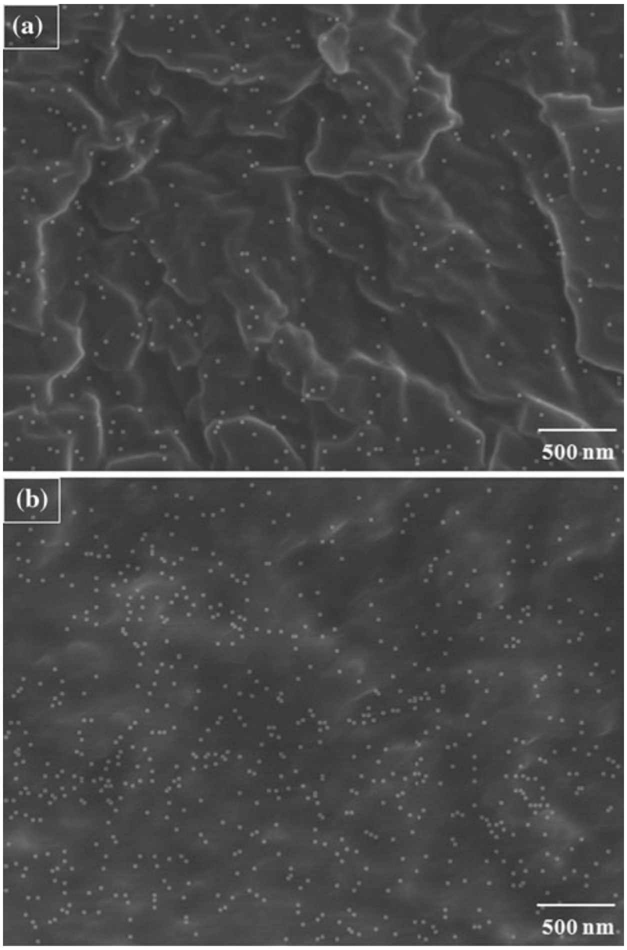

Fig. 2 X-ray EDX mapping analysis of **a** NyAB 0.5 and **b** NyAB 2 nanohybrids

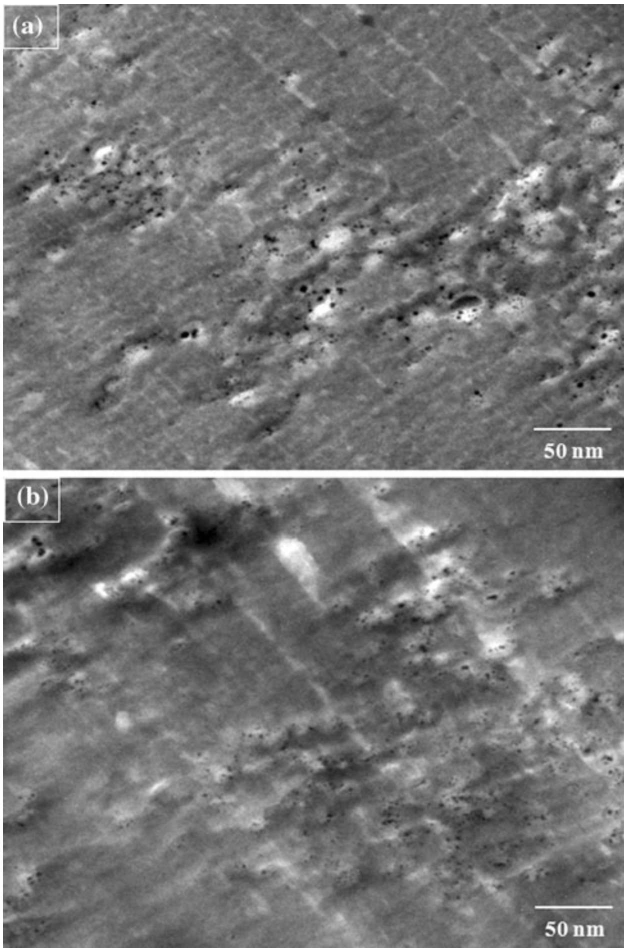

Fig. 3 FE-TEM images of **a** NyAB 0.5 and **b** NyAP 0.5 nanohybrids

FE-SEM. The FE-SEM images of the NyAB 0.5 (the number refers to the weight percent of POSS) and NyAB2 nanohybrids in Fig. 2 show filled circles corresponding to a Si-rich zone, indicating a uniform and fine dispersion of POSS domains. The weight percentage of Si obtained from the EDX analysis was similar throughout the entire Nylon 6 matrix, indicating that the dispersion of POSS is homogeneous. The Nylon 6 nanohybrids were also characterized on the nanometer scale using FE-TEM. As shown in Fig. 3, the FE-TEM images of the NyAB0.5 and NyAP0.5 nanohybrids showed dark zones that coincided with the POSS-rich zones due to the higher electron density of silicon atoms. A uniform and fine dispersion of POSS in the Nylon 6 matrix was also observed.

Melting point depression and interaction parameter determination

The thermodynamic interaction parameter, χ, is an important measure of the solubility of polymers in solvents and of the compatibility between pairs of chemical species such as polymer–polymer and polymer–nanoparticle combinations. The χ can be obtained from a range of experimental methods, such as an analysis of the melting point depression [3, 35], or a comparison of the solubility parameters [4], heats of mixing [36], cloud points [37], light scattering data [38], osmotic pressures [39], recoil spectrometry calculations [40], and inverse gas chromatography measurements [41].

Nishi and Wang [35], in their analysis of the decrease in melting temperature of a crystalline polymer in the presence of an amorphous one, derived a simple equation that relates the melting point depression directly to the interaction parameter as follows.

$$T_{\mathrm{m}}^{0} - T_{\mathrm{mix}}^{0} = -B\frac{V_{\mathrm{iu}}}{\Delta H_{\mathrm{iu}}}T_{\mathrm{m}}^{0}(1-\phi_{\mathrm{i}})^{2} \qquad (1)$$

where T_{m}^{0} and T_{mix}^{0} are the equilibrium melting temperatures of the semicrystalline polymer and mixture, respectively, $\Delta H_{\mathrm{iu}}/V_{\mathrm{iu}}$ is the heat of fusion of the semicrystalline polymer per unit volume, ϕ_{i} is the volume fraction of the

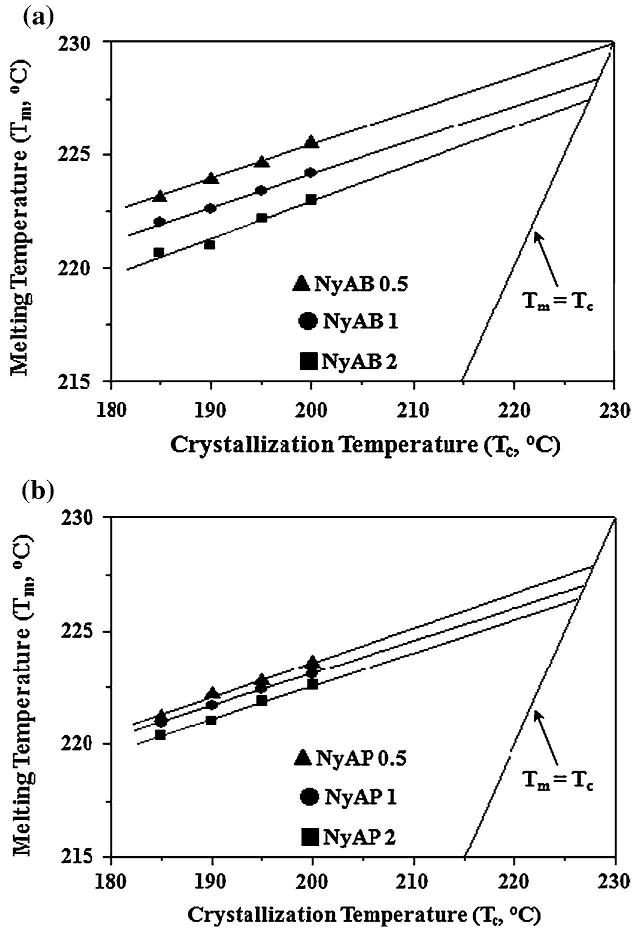

Fig. 4 Hoffman–Weeks plots of **a** NyAB and **b** NyAP nanohybrids

semicrystalline polymer, and B is the interaction parameter between the two components. The negative value of B for the binary system indicates that the two chemical species make a thermodynamically stable and compatible mixture. As shown in Fig. 4, the equilibrium melting temperatures of the pure Nylon 6 and Nylon 6/POSS nanohybrids were obtained using the Hoffman–Weeks plots and are listed in Table 1.

Figure 5 shows the melting point depression of Nylon 6 in the Nylon 6/POSS nanohybrids as a function of the Nylon 6 content. According to Eq. 1, the B values for the Nylon 6/POSS nanohybrids were determined from the slope of a straight line of Fig. 5. When the values of 104.2 cm^3 mol^{-1} and 7241.9 cal mol^{-1} were used for V_{iu} and ΔH_{iu}, respectively, the estimated thermodynamic interaction energy densities were −0.417, −0.357, and −0.238 cal cm^{-3} for B_{NyAB}, B_{NyAO}, and B_{NyAP}, respectively, suggesting that the Nylon 6 with ABPOSS is the most thermodynamically favorable.

The thermodynamic interaction between Nylon 6 and the POSS-derivatives was further predicted using the solubility parameter, δ, which is the square root of the cohesive energy density (the energy of vaporization per unit volume). Calculations based on group contributions were used for the solubility parameters of the polymers because it was not possible to obtain the molar vaporization energies for the polymers. There are several tables showing the molar attraction constants that can be used to calculate the solubility parameters [38]. In general, the Small and Hoy method is used to compute the solubility parameter due to its simplicity. However, it was assumed that no specific forces, such as a dispersion force, polar force and hydrogen bonding, are active between the structural units of the substances involved. Therefore, the Small and Hoy method is unsuitable for crystalline polymers. In this study, the solubility parameter of Nylon 6 and POSS-derivatives was calculated using the following equation according to the Hoftyzer and van Krevelen method [42].

$$\delta_{\mathrm{d}} = \frac{\sum F_{\mathrm{di}}}{V}, \quad \delta_{\mathrm{p}} = \frac{\sqrt{\sum F_{\mathrm{pi}}^2}}{V}, \quad \delta_{\mathrm{h}} = \sqrt{\frac{\sum E_{\mathrm{hi}}}{V}} \tag{2}$$

$$\delta_{\mathrm{t}}^2 = \delta_{\mathrm{d}}^2 + \delta_{\mathrm{p}}^2 + \delta_{\mathrm{h}}^2 \tag{3}$$

where δ_{d}, δ_{p}, and δ_{h} are the dispersion, polar, and hydrogen bonding components of the solubility parameter, respectively. F_{di} and F_{pi} are the dispersion and polar portions of the molar attraction constant. The F-method is not applicable to the calculation of δ_{h}. Hansen has already stated that the hydrogen bonding energy E_{hi} per structural group is relatively constant, which leads to the form of Eq. 2. For molecules with several planes of symmetry, $\delta_{\mathrm{h}} = 0$. Two assumptions were made to calculate the solubility parameters of polymers and POSS using the Hoftyzer and van Krevelen method. POSS is inherently an organic/inorganic hybrid, and it is commonly believed that the inorganic part of the POSS does not react completely in organic materials. Therefore, it was assumed that the functional group in the outer part of the POSS dominates the solubility parameter, and the inorganic part with siloxane bonding of POSS was excluded from the calculation of the solubility parameter.

Table 1 Measured equilibrium melting temperatures for the Nylon 6/POSS nanohybrids

	Ny	NyAB			NyAO			NyAP		
wt%[a]	100/0	99.5/0.5	99/1	98/2	99.5/0.5	99/1	98/2	99.5/0.5	99/1	98/2
T^0_{mix} (°C)	231.1	229.9	228.4	227.4	228.6	227.8	226.4	227.9	227.0	226.4

[a] The weight percent of Nylon 6 and POSS

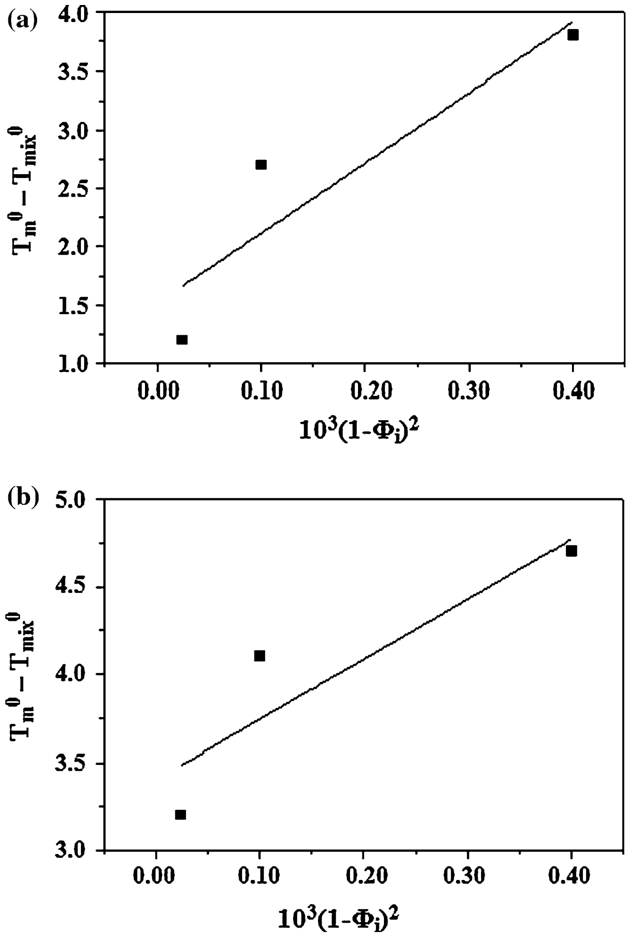

Fig. 5 Plots of the equilibrium melting points of Nylon 6 in the **a** NyAB and **b** NyAP nanohybrids

Table 2 lists the calculated solubility parameters for the polymers and POSS. For all polymers and POSS-derivatives in this study, the maximum difference in the solubility parameter showed the lowest value in the POSS functionalized with the isobutyl group. The meaning of the maximum difference of solubility parameter can be explained by Eq. 4, which interrelates the thermodynamic terms [42, 43].

$$\chi_{AB} = \frac{V_r}{RT}(\delta_A - \delta_B)^2 \tag{4}$$

where χ_{AB} is the Flory–Huggins interaction parameter of polymer A and POSS B, R and T are the gas constant and temperature, and V_r is the reference volume which is the molar volume of the smallest repeat unit. Therefore, it is expected that the interaction between Nylon 6 and POSS functionalized with an isobutyl group would be more thermodynamically favorable than the others. These results corresponded to the result based on the melting point depression method.

Activation energy

The activation energy of the polymer/POSS nanohybrids was estimated by using the Kissinger's equation shown below [44].

$$\ln\frac{\beta}{T_{\max}^2} = \left\{\ln\frac{AR}{E} + \ln\left[n(1-\alpha_{\max})^{n-1}\right]\right\} - \frac{E}{RT_{\max}} \tag{5}$$

where β is the heating rate (K min^{-1}), $T_{\max}$ is the temperature corresponding to the inflection point of the thermal degradation curve at the maximum degradation rate, A is the pre-exponential factor, $\alpha_{\max}$ is the maximum conversion, and n is the reaction order. $T_{\max}$ was determined from the differential TGA curves. Figure 6 shows plots of $\ln(\beta T_{\max}^{-2})$ versus $1/T_{\max}$ according to Kissinger's method for the Nylon 6 and Nylon 6/POSS nanohybrids containing 0.5 wt% POSS. The activation energies of the Nylon 6, NyAB, NyAO, and NyAP nanohybrids, which were calculated from the slope of the straight line in Fig. 6, were 2.49, 5.91, 4.82, and 4.16 kJ mol^{-1}, respectively. The

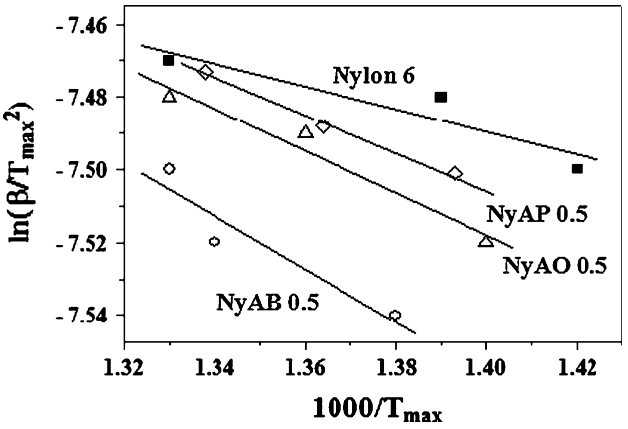

Fig. 6 Determination of the activation energies for the neat Nylon 6 and Nylon 6 nanohybrids

Table 2 Solubility parameters of Nylon 6 and POSS-derivatives

	F_d (J$^{1/2}$ cm$^{3/2}$ mol^{-1})	F_p (J$^{1/2}$ cm$^{3/2}$ mol^{-1})	E_h (J mol^{-1})	V (cm^3 mol^{-1})	δ_d (J$^{1/2}$ cm$^{-3/2}$)	δ_p	δ_h	δ
Ny	450	980	5100	28.3	15.9	34.6	13.4	18.0
AB	1190	0	0	68.2	17.5	0	0	17.5
AO	2870	0	0	154.4	18.6	0	0	18.6
AP	1430	110	0	74.5	19.2	1.5	0	19.3

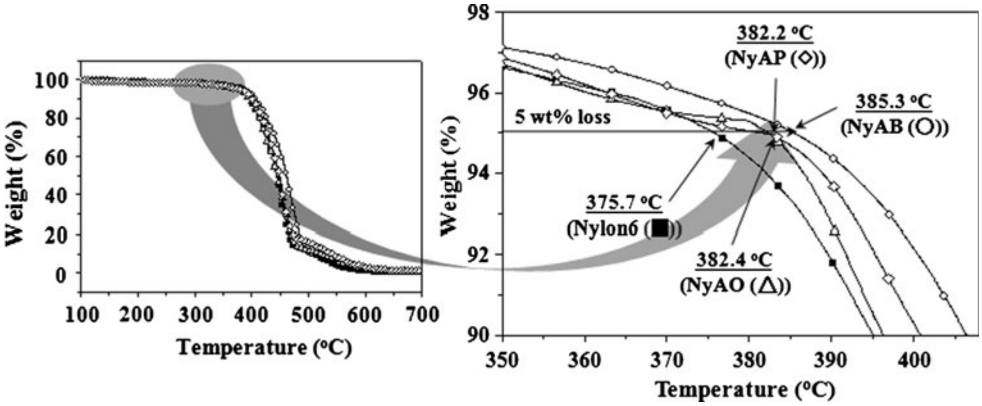

Fig. 7 TGA thermograms of the neat Nylon 6 and Nylon 6 nanohybrids. The POSS content was fixed at 0.5 wt%

NyAB nanohybrid showed the highest activation energy, meaning that the ABPOSS was dispersed most uniformly throughout the Nylon 6 matrix due to the increased interaction between Nylon 6 and ABPOSS.

Thermal and mechanical properties

The thermal and mechanical properties of Nylon 6/POSS nanohybrids were also analyzed for comparison of their theoretical and experimental results. Figure 7 shows the thermal decomposition temperatures (5 wt% loss) of the Nylon 6/POSS nanohybrids examined by TGA. As shown in Fig. 7, the decomposition temperatures of the nanohybrids were higher than that of Nylon 6, demonstrating that the thermal stability of nanohybrids is enhanced considerably by the incorporation of inorganic POSS [45–47]. Among the nanohybrids, the decomposition temperature of the NyAB nanohybrid was higher than that of the NyAO and NyAP nanohybrids. This might be due to the fact that the oxidation of the alkyl-substituted POSS in air occurs on the organic chains, which leads to a cage crosslinking to produce a ceramic silica-like phase [48].

Being independent of the type of POSS, the mechanical properties of the nanohybrids were higher than those of the neat Nylon 6, as shown in Fig. 8. The results showed that the proper incorporation of POSS could effectively enhance the mechanical properties of the Nylon 6 resin [46, 49]. In addition, the maximum tensile strength, tensile modulus, and elongation at break were obtained in the NyAB nanohybrid, indicating that the interaction between Nylon 6 and alkyl-substituted POSS is more favorable than that of NyAO and NyAP.

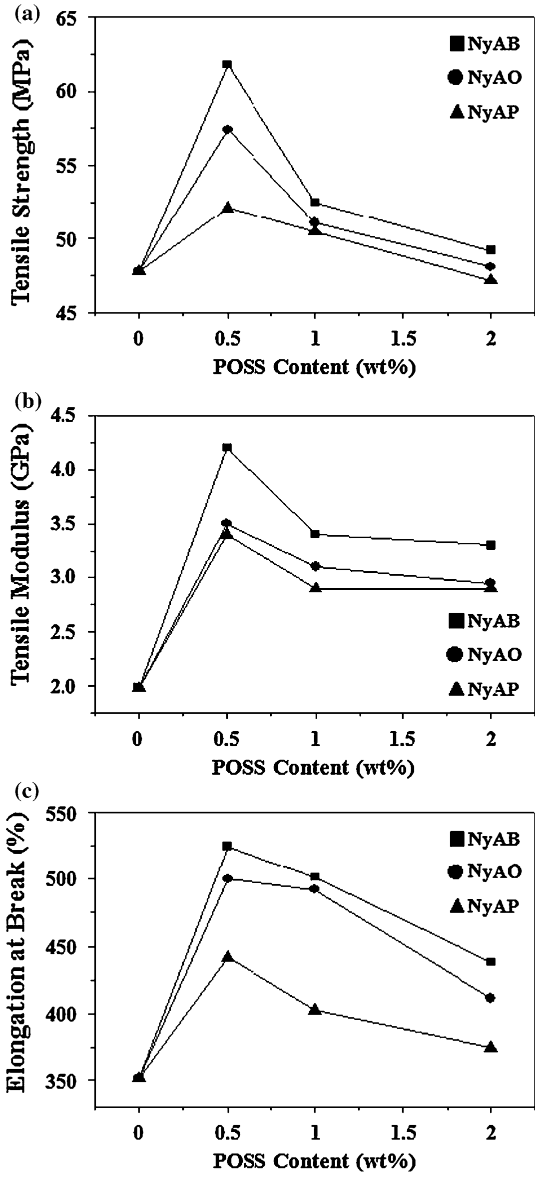

Fig. 8 **a** Tensile strength, **b** tensile modulus, and **c** elongation at break of Nylon 6/POSS nanohybrids

Conclusion

The thermodynamic interaction energy densities, *B* values, between Nylon 6 and POSS-derivatives in a Nylon 6/POSS nanohybrid were determined using the melting point depression method. The B values were -0.417, -0.357, and $-0.238\ \mathrm{cal\ cm^{-3}}$ for B_{NyAB}, B_{NyAO}, and B_{NyAP}, respectively, suggesting that the thermodynamic interaction between Nylon 6 and ABPOSS is the most favorable. The solubility parameter of Nylon 6 and the POSS-derivatives was calculated using the Hoftyzer and van Krevelen method to examine the thermodynamic interaction between the pairs. Based on the calculated values of the Flory–Huggins interaction parameters, Nylon 6 and ABPOSS were quite compatible, whereas NyAO and NyAP were less so. The activation energy data also indicated a better association between the Nylon 6 matrix and ABPOSS than that between Nylon 6 and the NyAO and NyAP nanohybrids. The thermal and mechanical properties of the Nylon 6 nanohybrids corresponded well with the results based on the thermodynamic interaction energy density, solubility parameter calculation, and activation energy.

Acknowledgement The financial support of this study by the Brain Korea 21 Project in 2009 is greatly acknowledged.

References

1. Alexandre M, Dubois P (2000) Mater Sci Eng Rep 28:1
2. Potschke P, Pegel S, Claes M, Bonduel D (2008) Macromol Rapid Commun 29:244
3. Lim SK, Kim JW, Chin IJ, Kwon YK, Choi HJ (2002) Chem Mater 14:1989
4. Lim SK, Lee EH, Chin IJ (2008) J Mater Res 23:1168
5. Liu YD, Fang FF, Choi HJ (2011) Soft Matter 7:2782
6. Zhang WL, Liu YD, Choi HJ (2011) J Mater Chem 21:6916
7. Park BJ, Fang FF, Choi HJ (2010) Soft Matter 6:5246
8. Li G, Wang L, Ni H, Pittman CU (2001) J Inorg Organomet Polym 11:123
9. Sanchez C, Soler-Illia GJDA, Ribot F, Lalot T, Mayer CR, Cabuil V (2001) Chem Mater 13:3061
10. Pielichowski K, Njuguna J, Janowski B, Pielichowski J (2006) Adv Polym Sci 201:225
11. Xie P, Zhang R (1997) Polym Adv Technol 8:649
12. Lichtenhan JD (1995) Comments Inorg Chem 17:115
13. Park JY, Kim MG, Kim JB (2008) Macromol Rapid Commun 29:1532
14. Deng JJ, Polidan JT, Hottle JR, Farmer-Creely CE, Viers BD, Esker AR (2002) J Am Chem Soc 124:15194
15. Haddad TS, Lichtenhan JD (1996) Macromolecules 29:7302
16. Schwab JJ, Lichtenhan JD (1998) Appl Organomet Chem 12:707
17. Choi J, Harcup J, Yee AF, Zhu Q, Laine RM (2001) J Am Chem Soc 123:11420
18. Zheng L, Waddon AJ, Farris RJ, Coughlin EB (2002) Macromolecules 35:2375
19. Constable GS, Lesser AJ, Coughlin EB (2004) Macromolecules 37:1276
20. Cardoen G, Coughlin EB (2004) Macromolecules 37:5123
21. Verker R, Grossman E, Gouzman I, Eliaz N (2009) Compos Sci Technol 69:2178
22. Wu J, Haddad TS, Mather PT (2009) Macromolecules 42:1142
23. Somboonsub B, Thongyai S, Praserthdam PJ (2009) Appl Polym Sci 114:3292
24. Tsuchida A, Bolln C, Sernetz FG, Frey H, Mulhaupt R (1997) Macromolecules 30:2818
25. Zheng L, Farris RJ, Coughlin EB (2001) J Polym Sci A 39:2920
26. Li GZ, Cho H, Wang L, Toghiani H, Pittman CU (2005) J Polym Sci A 43:355
27. Ohno K, Sugiyama S, Koh K, Tsujii Y, Fukuda T, Yamahiro M, Oikawa H, Yamamoto Y, Ootake N, Watanabe K (2004) Macromolecules 37:8517
28. Turri S, Levi M (2005) Macromolecules 38:5569
29. Hato MJ, Ray SS, Luyt AS (2010) Adv Sci Lett 3:123
30. Hato MJ, Ray SS, Luyt AS (2008) Macromol Mater Eng 293:752
31. Lim SK, Hong EP, Song YH, Choi HJ, Chin IJ (2010) J Mater Sci 45:5984. doi:10.1007/s10853-010-4446-z
32. Li Q, Xu Y, Yoon JS, Chen GX (2011) J Mater Sci 46:2324. doi:10.1007/s10853-010-5077-0
33. Riedl BJ, Prud'homme RE (1984) Polym Eng Sci 24:1291
34. Csaki KF, Nagy M, Csempesz F (2005) Langmuir 21:761
35. Nishi T, Wang TT (1975) Macromolecules 8:909
36. Barlow JW, Paul DR (1987) Polym Eng Sci 27:1482
37. Kim CK, Paul DR (1992) Polymer 33:1630
38. Fukuda T, Nagata M, Inagaki H (1984) Macromolecules 17:548
39. Shiomi T, Kohno K, Yoneda K, Tomita T, Miya M, Imai K (1985) Macromolecules 18:414
40. Green PF, Doyle BL (1986) Phys Rev Lett 57:2407
41. Olabisi O (1975) Macromolecules 8:316
42. van Krevelen DW (1990) Properties of polymers. Elsevier, New York
43. Jang BN, Wang D, Wilkie CA (2005) Macromolecules 38:6533
44. Kissinger HE (1957) Anal Chem 29:1702
45. Mather PT, Jeon HG, Romo-Uribe A, Haddad TS, Lichtenhan JD (1999) Macromolecules 32:1194
46. Liang K, Li G, Toghiani H, Koo JH, Pittman CU (2006) Chem Mater 18:301
47. Lim SK, Hong EP, Choi HJ, Chin IJ (2010) J Ind Eng Chem 16:189
48. Fina A, Tabuani D, Carniato F, Frache A, Boccaleri E, Caminoa G (2006) Thermochim Acta 440:36
49. Wang J, Ye Z, Joly H (2007) Macromolecules 40:6150